Exploring the Extent of Magnetic Field Effect on Intermolecular Photoinduced Electron Transfer in Different Organized Assemblies

Sharmistha Dutta Choudhury and Samita Basu*

Chemical Sciences Division, Saha Institute of Nuclear Physics, 1/AF, Bidhannagar, Kolkata 700 064, India

Received: June 15, 2005; In Final Form: July 25, 2005

Magnetic field effect (MFE) on the photoinduced electron transfer (PET) between phenazine (PZ) and the amines, *N*,*N*-dimethylaniline , *N*,*N*-diethylaniline, 4,4′-bis(dimethylamino)diphenylmethane (DMDPM), and triethylamine, has been studied in micelles, reverse micelles, and small unilamellar vesicles (SUVs) with a view to understand the effect of spatial location of the donor and acceptor moieties on the magnetic field behavior. The structure of the assembly is found to influence greatly the PET dynamics and hence the MFE of all the systems studied. The magnetic field behavior in micelles is consistent with the hyperfine mechanism, but high $B_{1/2}$ values have been obtained which have been ascribed to hopping and lifetime broadening. The variation of MFE with W_0, in reverse micelles, proves yet again that the MFE maximizes at an optimum separation distance between the acceptor and donor. This is the first example of such behavior for intermolecular PET in heterogeneous medium. We have also reported for the first time MFE on intermolecular PET in SUVs. In this case, the PZ−DMDPM system responds most appreciably to an external field compared to the other acceptor−donor systems because it is appropriately positioned in the bilayer. The differential behavior of the amines has been discussed in terms of their confinement in different zones of the organized assemblies depending on their bulk, hydrophobic, and electrostatic effects.

Introduction

Photoinduced electron transfer (PET) reactions involve the formation of radical ion pairs (RIPs) and in general can be affected by an external magnetic field.[1−5] Magnetic field effect (MFE) is basically interplay between spin dynamics and diffusion dynamics. By diffusion, the RIPs can separate to an optimum distance where the exchange interaction $J \approx 0$. In this situation, the electron−nuclear hyperfine coupling induces efficient mixing between the triplet ($T_{\pm}$, T_0) and the singlet (S) states. The application of an external magnetic field removes the degeneracy of the triplet states and reduces intersystem crossing thus resulting in an increase in the population of the initial spin state. So the MFE is very sensitive to the distance between the participating radical ions because the hyperfine induced spin flipping depends on *J*, which in turn has exponential distance dependence. When the RIP is in contact, the S−T splitting caused by *J* is much stronger than the hyperfine coupling energies so that spin evolution cannot occur by this mechanism. On the other hand, at a distance where *J* is sufficiently small and S−T conversion can occur, the separation of the two radicals may be already too far for geminate recombination to occur. Therefore the requirement of an optimum separation such that both spin flipping and recombination are feasible becomes a very crucial factor in controlling the MFE. This distance dependence of MFE has been demonstrated earlier in a detailed and quantitative manner by several workers using covalently linked acceptor−donor systems.[5−7]

In this work, we have attempted to investigate this aspect by studying the MFE on PET between several unlinked acceptor−donor systems in different organized assemblies, namely, micelles, reverse micelles, and small unilamellar vesicles (SUVs). The participating molecules are expected to reside in different zones of the organized assemblies with different local environments, and this spatial organization should be reflected in the magnetic field behavior. Therefore the organized assemblies act qualitatively as an alternative to linked systems. The MFE can also be used as a tool to probe the PET reactions and the properties of the local environment sensed by the radical ions and hence to predict the preferential location of the acceptor and donor molecules.

PET reactions in organized assemblies have been extensively studied and continue to attract the attention of the scientific community. Interests in research on such systems are manifold. For proper utilization of PET, the photogenerated ions should be prevented from subsequent rapid recombination, a prevalent event in homogeneous media. Organized assemblies such as micelles, reverse micelles, and vesicles have the potential to prolong the lifetime of charge-transfer states and thus increase the efficiency of charge separation by partitioning of the reactants and/or products.[8] These microheterogeneous systems provide a fundamental understanding of how PET dynamics is influenced by restricted system geometry. Moreover, understanding PET in simple organized assemblies can lead to a better understanding of similar processes in biological systems.

In this work, we have studied the PET between phenazine (PZ) and some amines, *N*,*N*-dimethylaniline (DMA), *N*,*N*-diethylaniline (DEA), 4,4′-bis(dimethylamino) diphenylmethane (DMDPM), and triethylamine (TEA) for comparison. We have earlier reported exciplex formation between PZ and the aromatic amines, DMA, DEA, and DMDPM.[9] We have also used laser flash photolysis to identify the transients formed by PET from the aromatic amines to PZ and revealed the different nature of the complexation of PZ with DMA and DMDPM.[10] For triplet derived RIPs, as in the present systems under study, the MFE is not observed in homogeneous systems. This is because radical

* To whom correspondence should be addressed. E-mail: samita.basu@saha.ac.in. Tel: +91 033 23375345. Fax: +91 033 23374637.

10.1021/jp053222y CCC: $30.25
Published on Web 08/23/2005

separation is so rapid that the geminate reaction is generally a very minor process. On the other hand, in organized assemblies, the RIPs are compartmentalized in the restricted environment and can retain their geminate character for a sufficiently long time so that spin flipping can occur.[11] Hence, a distinct MFE is observed. There have been some studies of MFE on PET reactions in micelles and reverse micelles.[1−5,12−18] MFE has also been studied for intramolecular PET[19] and photogenerated radicals in SUVs.[20] However, there has been no report so far for the observation of MFE in SUVs on intermolecular PET where donor and acceptor molecules undergo free diffusion. Ours is the first such report.

Experimental Section

Materials. PZ and DMDPM were obtained from Aldrich and were recrystallized from ethanol. DMA, DEA, and TEA were obtained from Sisco Research Laboratories and were used after proper distillation. UV spectroscopy grade chloroform (CF), ethanol (EtOH), and methanol (MeOH) were obtained from Spectrochem and used as such without purification. Tris buffer was obtained from Spectrochem. Heptane (HP) and benzene (BZ) were obtained from Merck (Uvasol). Sodium dodecyl sulfate (SDS), sodium bis(2-ethylhexyl)sulfosuccinate (AOT), and D,L-dimyristoyl-α-phosphatidylcholine (DMPC) from Sigma and benzyldimethylhexadecylammonium chloride (BHDC) from Fluka were used as such. Water was triply distilled.

Methods. Preparation of Micelles and Reverse Micelles. Aqueous 10% SDS micellar solutions containing PZ (1×10^{-4} M) and the respective amines (8×10^{-3} M) were prepared by sonication. AOT (0.05−0.2 M) and BHDC (0.2 M) reverse micelles were prepared in HP and BZ solvents, respectively.[21−23] The final concentration of PZ was 1×10^{-4} M and that of the amines was 2×10^{-2} M in both cases. The desired amount of water was added for W_0 variation ($W_0 = [H_2O]$/molar concentration of the reverse micelle).

Preparation of SUVs. SUVs of DMPC were prepared by the method of sonication.[24] The phospholipid was first dissolved in a 2:1 (v/v) CF/MeOH solution in a glass tube, and the solvent was evaporated under a stream of Ar. The resultant lipid film was then dried overnight in a vacuum desiccator at −20 °C. The dry film was hydrated and swelled in Tris buffer at pH 7.8, and the mixture was vortexed to disperse the lipids. The dispersion was then sonicated using a Lab Plant Ultrason 250 probe sonicator (90% pulse cycle). The samples were then allowed to stand for 30 min for complete hydration. The sonicated samples were centrifuged at 10 000 rpm for 15 min to remove titanium particles originating from the sonicator probe. PZ solution in Tris buffer was added prior to sonication so that the final concentration of PZ was 1×10^{-4} M. EtOH solutions (EtOH was 5% of the total volume) of DEA, DMA, and TEA were also added to the solution prior to sonication so that the final concentration of the amines was 8×10^{-3} M. DMDPM was added to the CF/MeOH mixture prior to formation of the film. The concentration of DMDPM in the sample was found to be 7.2×10^{-4} M by absorbance (OD) measurement. DMPC concentration was kept at 0.01 M in each set. Freshly prepared vesicle dispersions were used throughout this work, and experiments were performed at room temperature, which was above the phase transition temperature of DMPC.

Transient absorption spectra were measured using a nanosecond flash photolysis setup (Applied Photophysics) containing an Nd:YAG laser (DCR−II, Spectra Physics). The sample was excited by 355 nm laser light (fwhm = 8 ns). Transients were monitored through absorption of light from a pulsed Xe lamp (250 W). The photomultiplier (IP28) output was fed into a combiscope (Fluke PM3394B, 200 MHz), and the data was analyzed using Fluke View combiscope software (SW33W). MFE on the transient absorption spectra was studied by passing dc through a pair of electromagnetic coils placed inside the sample chamber. The software Origin 5 was used for curve fitting. All samples were deaerated by passing pure Ar gas prior to experiment. No degradation of the samples was observed during the experiment.

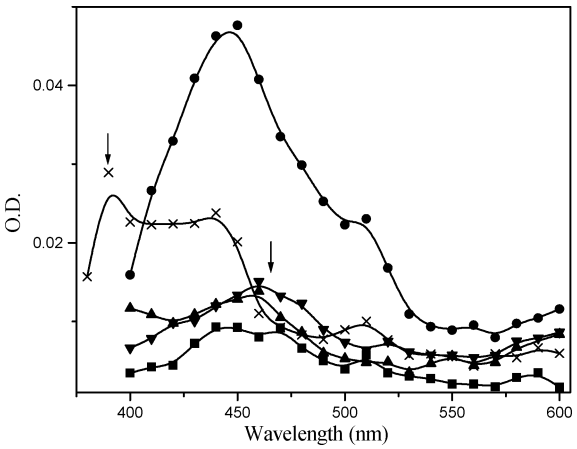

Figure 1. Transient absorption spectra of PZ (1×10^{-4} M) (●), PZ (1×10^{-4} M)−DMA (8×10^{-3} M) (▲), PZ (1×10^{-4} M)−DEA (8×10^{-3} M) (▼), PZ (1×10^{-4} M)−DMDPM (8×10^{-3} M) (■), and PZ (1×10^{-4} M)−TEA (8×10^{-3} M) (×) in 10% SDS solution at 0.8 μs after the laser flash with excitation wavelength 355 nm. The positions of the radical cations (∼460 nm and ∼380 nm) are marked by arrows.

Results and Discussion

In our earlier work, we have observed that the triplet−triplet absorption spectrum of PZ has a peak at 440 nm, which tallies with the literature.[25] On addition of the amines, we have also found that this peak is quenched and new peaks arise due to formation of radical ions. The radical cations of DMA, $DMA^{\bullet+}$, and DMDPM, $DMDPM^{\bullet+}$, are observed around 460 and 480 nm respectively.[10] From the literature we have noted that $DEA^{\bullet+}$ and $TEA^{\bullet+}$ absorb around 460[26] and 380 nm,[27] respectively. The radical anion of PZ, $PZ^{\bullet-}$, absorbs around 550 nm[25] but was not observed in our spectrum probably because it was masked by the radical cation absorptions.

MFE in SDS Micelles. A micelle typically forms as an approximately spherical structure in which a hydrophobic inner core is separated from the surrounding polar solution by a shell comprised of the headgroups and their accompanying solvation shells.[8] The basic requirement for observation of MFE is ideally fulfilled in micellar aggregates, and much work has been done by the groups of Turro, Hayashi, Tanimoto, and Scaiano.[1−5,11−13] However, most of the investigations have involved neutral radical pairs produced in reactions of excited carbonyl triplets by hydrogen atom transfer or by homolytic α C−C bond cleavage in aliphatic ketones. Examples of MFE on PET reactions are less numerous. Tanimoto et al. first observed MFE on PET from diphenylamine to triplet duroquinone and 1-acetonaphthone.[12,13] Later on, several other workers have reported MFE on both intra- and intermolecular PET in micelles, and studies have been extended to very high fields as well. Our laboratory has reported MFE on the *N*-ethylcarbazole-1,4-dicyanobenzene exciplex in micelles.[28,29] In this work too we have observed a profound MFE for all the acceptor−donor pairs in micelle.

Figure 1 shows the transient absorption spectra of pure PZ (1×10^{-4} M) and PZ with the amines (8×10^{-3} M) in SDS.

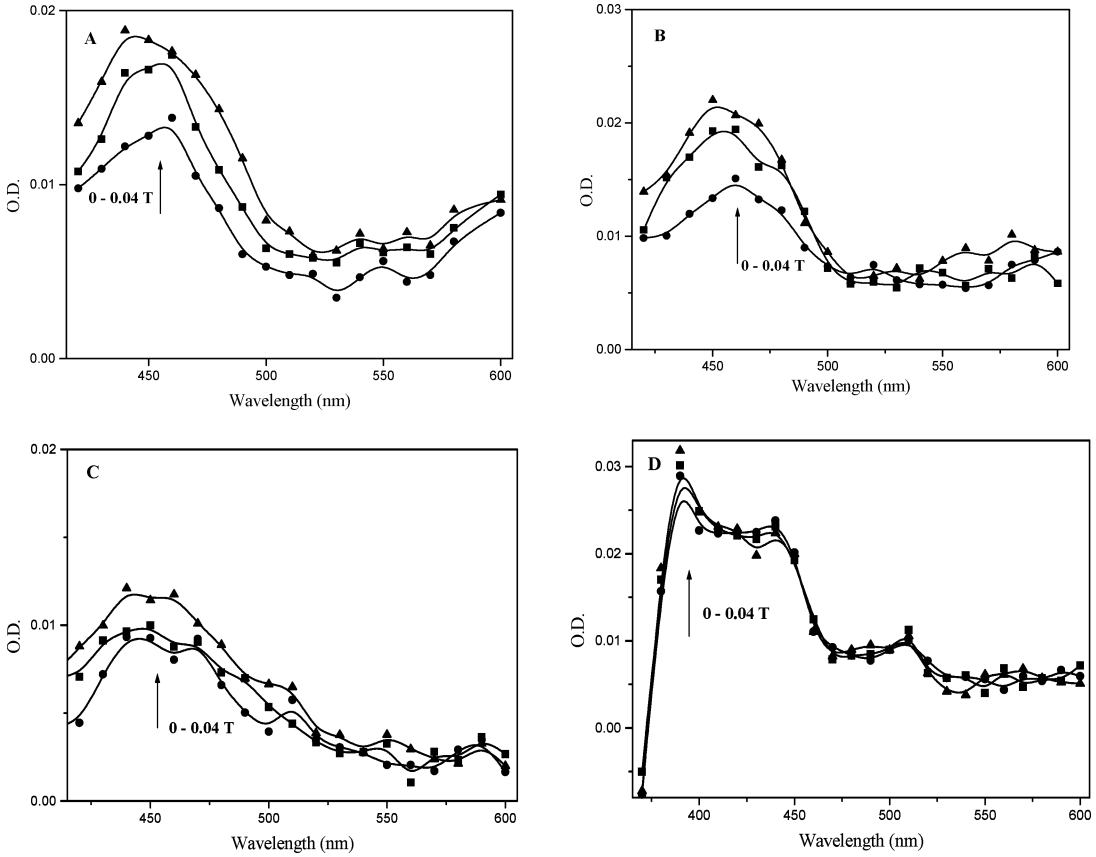

Figure 2. Effect of an external magnetic field, 0 T (●), 0.02 T (■), and 0.04 T (▲) on the transient absorption spectra of (A) PZ (1×10^{-4} M)−DMA (8×10^{-3} M), (B) PZ (1×10^{-4} M)−DEA (8×10^{-3} M), (C) PZ (1×10^{-4} M)−DMDPM (8×10^{-3} M), and (D) PZ (1×10^{-4} M)−TEA (8×10^{-3} M) at 0.8 μs after the laser flash in 10% SDS solution with excitation wavelength 355 nm.

The transient absorption of PZ is considerably quenched on addition of the amines in comparison to homogeneous solutions. This may be due to some contribution from static quenching involving preformed PZ−amine aggregates. Characteristic peaks are observed in the 460−480 nm region due to the radical cations of DMA, DEA, and DMDPM. Atik and Thomas have earlier reported that the yield of radical ions decreases with increasing rigidity or viscosity of the medium, that is, in going from a spherical to rodlike micelle, due to restricted mobility.[30] This may also be the reason for the low absorption of the radical cations observed in our case, since we have performed our experiments at 10% SDS concentration when cylindrical micelles are formed.[31]

Figure 2A shows the effect of an external magnetic field on the transient absorption spectrum of PZ (1×10^{-4} M)−DMA (8×10^{-3} M). It is seen that the transient absorption increases on increasing the field from 0 to 0.04 T especially in the region of $DMA^{\bullet+}$ at 460 nm. Similar behavior is also observed for PZ−DEA (Figure 2B), PZ−DMDPM (Figure 2C), and PZ−TEA (Figure 2D). However the effect is very small in the case of TEA.

The decay of RIP in micellar solution is expected to be biexponential. The change in absorbance $A(t)$ follows the expression, $A(t) = I_f \exp(-k_f t) + I_s \exp(-k_s t)$, where k_f and k_s are the rate constants for the fast and slow components of the decay profiles, respectively.[32] The fast component corresponds to the decay in the micellar cage, and the slower one corresponds to the reaction of the escaped radicals. The k_f values obtained by biexponential fitting of the decay profiles of all the acceptor−donor systems are listed in Table 1. The yields of the radical ions in the bulk of the solvent may be obtained from the ratio of the absorption due to the free radical ions to that of the initial absorption immediately after the pulse. The relative escape yields after 5 μs are also presented in Table 1. It is observed that with increasing field, the decay rate decreases and correspondingly the escape yield increases. This implies that the RIPs are generated in the triplet spin state. Upon application of a magnetic field, the conversion of the triplet RIP to the singlet RIP is retarded, and consequently, the decay rates are decreased and escape yield is increased.

TABLE 1: Variation of Rate Constants (k_f) and Relative Radical Escape Yield after 5 μs (Y), with Different External Magnetic Field in 10% SDS Solution

system	magnetic field (T)	$k_f \times 10^{-6}$ (s^{-1})	Y
PZ−DMA	0.00	2.22	1.00[a]
	0.02	1.40	1.38
	0.04	0.96	1.59
PZ−DEA	0.00	1.28	1.00[a]
	0.02	1.12	1.20
	0.04	1.07	1.86
PZ−DMDPM	0.00	1.94	1.00[a]
	0.02	1.86	1.11
	0.04	1.65	1.12
PZ−TEA	0.00	0.11	1.00[a]
	0.02	0.08	1.09
	0.04	0.07	1.15

[a] Arbitrarily taken.

Figure 3 shows the variation of ΔOD with magnetic field (B) where, $\Delta OD(B) = OD(B) - OD$ ($B = 0$), is taken as a measure of the MFE. It is seen that ΔOD increases with an increase in field and then reaches saturation. MFEs on PET reactions have been interpreted in terms of Δg, hyperfine coupling, level crossing, relaxation, and triplet mechanisms.[1−5]

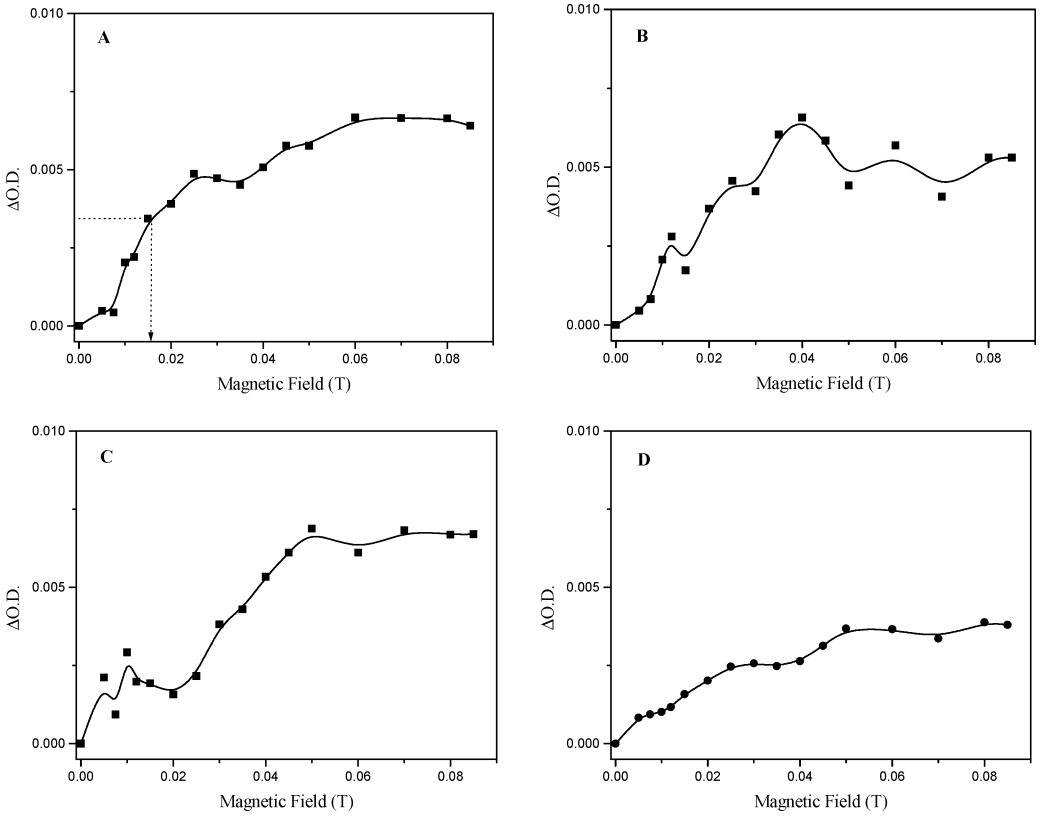

Figure 3. Variation of ΔOD with external magnetic field for (A) PZ (1×10^{-4} M)−DMA (8×10^{-3} M), (B) PZ (1×10^{-4} M)−DEA (8×10^{-3} M), and (C) PZ (1×10^{-4} M)−DMDPM (8×10^{-3} M) at 460 nm and (D) PZ (1×10^{-4} M)−TEA (8×10^{-3} M) at 380 nm in 10% SDS solution, 0.8 μs after the laser flash. The experimental $B_{1/2}$ value is shown in A as an illustration.

TABLE 2: Experimentally Obtained $B_{1/2}$ Values in 10% SDS Solution

system	$B_{1/2}$ (T)
PZ−DMA	0.015 ± 0.0005
PZ−DEA	0.017 ± 0.001
PZ−DMDPM	0.029 ± 0.001
PZ−TEA	0.019 ± 0.001

Our observations are consistent with the hyperfine coupling mechanism. The $B_{1/2}$ is the magnetic field required to attain half the saturation value for a particular system and is a measure of the hyperfine interaction present in the system. The experimentally obtained $B_{1/2}$ values are presented in Table 2.

$B_{1/2}$ values can also be theoretically calculated from the hyperfine coupling constants, a_{iN}, of the individual radical ions according to the model proposed by Weller and co-workers.[33] Values of a_{iN} for DMA and PZ were obtained from the literature,[34] and the $B_{1/2}$ for PZ−DMA was calculated to be 0.0050 T. The a_{iN} values for other amines were not available from the literature. However it is obvious that the experimentally obtained $B_{1/2}$ values are much higher than the expected values. The $B_{1/2}$ value for TEA, however, appears to be closer to the expected value since the calculated value for PZ−trimethylamine is 0.0143 T.[34] The disparity between the calculated and observed values is quite intriguing.

Deviation from calculated $B_{1/2}$ values have been observed earlier in homogeneous medium at high donor concentrations and have been ascribed to the hopping mechanism.[35] When the donor concentration is high, the unpaired electron spin at the cation radical may migrate between several donors in the vicinity before encountering the acceptor radical anion. The consequence of this hopping between donors differing in their nuclear spin configurations is a remarkable increase in the external magnetic field strength required to overcome the hyperfine interaction and the width of the electron spin levels to effectively decouple the T_+, T_- states from S and T_0. So hopping manifests itself in a lifetime broadening and leads to an increase in $B_{1/2}$. Sakaguchi et al. and Ulrich et al. have observed high $B_{1/2}$ values and saturation at very high fields in microheterogeneous media.[36,37] They have pointed out the role of diffusion and spin relaxation. Diffusion may limit the rate constant of recombination and higher fields are necessary to make spin relaxation, $T_\pm \rightarrow T_0$, S slow enough to show up in the geminate recombination kinetics.

We have performed our experiments in 10% SDS micellar solution, and at this concentration, the micelles have a cylindrical shape with high aggregation number, as mentioned before.[31] The aromatic amines that we have used as donors will preferably be located in the hydrophobic core of the micelle, and so the effective concentration of the donors may be expected to be quite high. This should promote electron hopping and lead to an increase in the $B_{1/2}$ value. We have tried to study the effect of donor concentration variation on the $B_{1/2}$ value, but within the experimentally feasible range of concentration (1×10^{-4} to 8×10^{-3} M), no appreciable change in $B_{1/2}$ was observed. The aliphatic amine, TEA, is less hydrophobic and probably remains in the bulk or near the interface. As a result, the effective concentration inside the micelle will be less, and consequently, no hopping will be possible. Thus a $B_{1/2}$ value that is close to the expected value is obtained. This is also in accordance with the small MFE observed for this system. Scaiano et al. have also not observed any MFE on the PET reaction between 2,3,6,7-dibenzofluorenone and TEA.[38] They have attributed this to the solubility of TEA and the corresponding radical in water, which results in rapid entry−exit equilibria with the micellar phase.

Besides hopping, another possible reason for the increase in $B_{1/2}$ could be lifetime broadening due to frequent reencounter

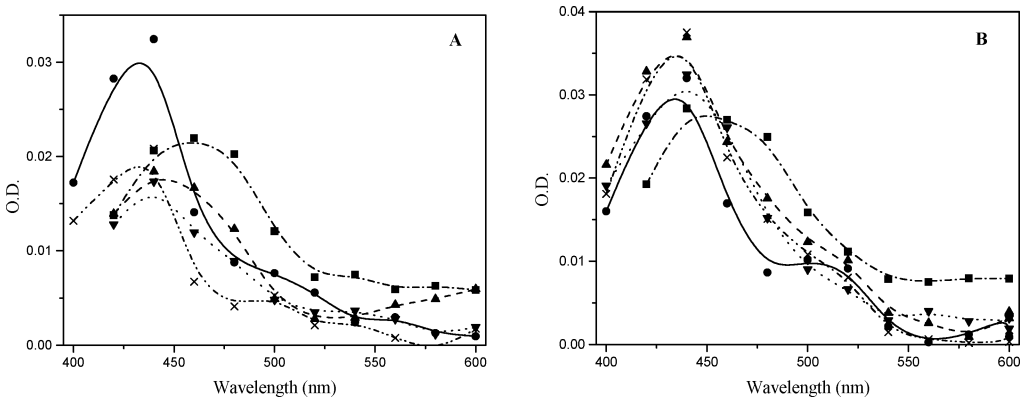

Figure 4. Transient absorption spectra of PZ (1×10^{-4} M) (●), PZ (1×10^{-4} M)−DMA (2×10^{-2} M) (▲), PZ (1×10^{-4} M)−DEA (2×10^{-2} M) (▼), PZ (1×10^{-4} M)−DMDPM (2×10^{-2} M) (■), and PZ (1×10^{-4} M)−TEA (2×10^{-2} M) (×) in (A) AOT (0.2 M) and (B) BHDC (0.2 M) reverse micelles at $W_0 = 20$, 0.8 μs after the laser flash of 355 nm.

within the RIP. Since the space available to the RIP is restricted, its separation will often be within the distance where the exchange interaction, *J*, cannot be neglected. Since we do not observe a level crossing effect as was observed by Weller et al. for a series of acceptor−donor systems linked by methylene units, we can conclude that in our case $J_{\text{effective}} < B_{1/2}$.[7] However, Weller et al. have found that $B_{1/2}$ values in linked RIPs with an interradical separation >10 Å may still be much larger than those for freely diffusing RIPs. This was attributed to the lifetime broadening of the linked RIPs due to frequent encounters, which reduces the time span available for free spin evolution. A situation similar to that of a linked acceptor−donor system could arise in the present case when the RIPs are sequestered inside the micelle, leading to an increase in $B_{1/2}$. The experimentally observed $B_{1/2}$ values follow the trend PZ−DMA < PZ−DEA < PZ−DMDPM which is expected since a_{iN} values for the aromatic amines should also follow the same order.

The lifetimes of the RIPs are greatly enhanced in the micellar cage, and as a result slow spin flip processes such as spin relaxation can greatly contribute to the multiplicity change of the RIP during intramicellar recombination process. Thus, although the hopping mechanism and lifetime broadening satisfactorily explain our observed results, the relaxation mechanism cannot be ruled out completely and studies with higher magnetic fields can provide some insight in this direction.

MFE in Reverse Micelles. Reverse micelles consist of a homogeneous thermodynamically stable solution of nanodroplets of water surrounded by a surfactant monolayer and dispersed in an organic solvent. Thus it is possible to localize the reactants and/or products in three different regions of the reverse micelle: the water pool, the micellar interface, and the organic bulk solvent.[21−23] PET in reverse micellar systems has been extensively studied. Different fluorescence quenching and radical ion yields have been observed depending on the location of the species and the charge of the surfactant.[39−43] MFE studies in these systems are few compared to the large volume of work done in micelles and were first reported by Steiner and co-workers for the thionine−aniline system in the AOT reverse micelle.[14,15] Their study elucidated the importance of diffusion dynamics of the RIPs. Later on Baumann et al.[16] and Uehata et al.[17] have reported MFE in reverse micelles. Recently, MFE has been observed in the exciplex luminescence of the pyrene−DMA system in reverse micelles, and the field effect has been used to estimate the polarity in the vicinity of the charge-transfer species.[18]

We have studied the MFE with our present systems in two types of reverse micelles, the anionic AOT and the cationic BHDC. Water/AOT/HP and water/BHDC/BZ reverse micelles are quite well-characterized in the literature.[21−23] Figure 4 shows the transient absorption spectra for all the different acceptor−donor systems in AOT and BHDC, respectively. We see that the peaks for the radical cations, $DMA^{\bullet+}$, $DEA^{\bullet+}$, and $DMDPM^{\bullet+}$, are all very prominent in AOT compared to BHDC. This can be explained by hydrophobic and electrostatic effects. PZ being hydrophobic will remain in the bulk or near the micellar tail region. DMA, DEA, and TEA being small molecules will tend to partition between the organic, micellar, and aqueous phases. The radical cations will be further stabilized by the anionic headgroup of AOT following charge transfer and so can be distinctly observed. In the case of BHDC, the positively charged headgroup will repel the radical cations so the charge stabilization is less and the radical cations are not distinctly observed in the spectrum. $DMDPM^{\bullet+}$, however, shows a distinct absorption in both the reverse micelles. We have earlier observed that the transient absorption of $DMDPM^{\bullet+}$ is not affected by the nature of the solvent.[10] Moreover, $DMDPM^{\bullet+}$ is a bulky organic ion, and therefore the electrical repulsion by the positive headgroup of BHDC is not large enough to expel the radical cation from the interface.

A small but distinct MFE was observed for PZ−DMA, PZ−DEA, and PZ−DMDPM in AOT reverse micelles. No MFE is observed for PZ−TEA probably due to rapid equilibrium of TEA between the different phases of the reverse micelle. Again, it has been found that the MFE increases with an increase in AOT concentration from 0.05 to 0.2 M. This can be explained by the caging effect. As AOT concentration increases, more and more reverse micelles are formed and the caging of the acceptor and donor inside the reverse micelle also increases. The caging effect is essential for increasing RIP lifetime for observation of this enhanced MFE.

Another interesting observation regarding the MFE dependence on distance is the peculiar behavior of the MFE with variation in the water pool size, W_0 (Figure 5). For a given concentration of AOT, the size of the entrapped water pool and hence that of the reverse micelle depends on the ratio between water and AOT molecules ($W_0 = [H_2O]/[AOT]$). The water pool size is given by $2W_0$ Å. [22] Thus the water pool sizes that we have studied are 10, 20, 40, and 80 Å corresponding to W_0 values of 5, 10, 20, and 40. We have seen that the MFE increases with an increase in W_0 and then decreases again. As mentioned earlier, the observation of MFE involves diffusion, spin flipping, and geminate recombination. When the participating radicals are close to each other (small W_0 values), the exchange interaction, *J*, will hinder spin conversion and at

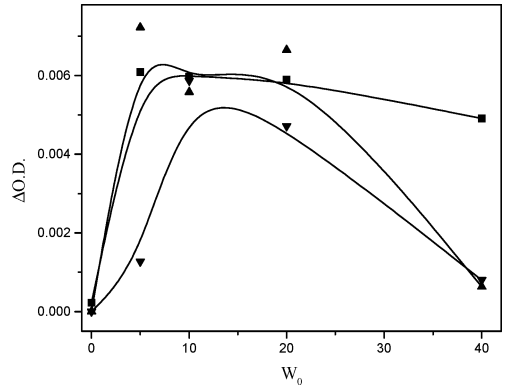

Figure 5. Variation of ΔOD (OD (0.1 T) − OD (0.0 T)) with W_0 for PZ (1×10^{-4} M)−DMA (2×10^{-2} M) (▲), PZ (1×10^{-4} M)−DEA (2×10^{-2} M) (▼), and PZ (1×10^{-4} M)−DMDPM (2×10^{-2} M) (■) in 0.2 M AOT reverse micelle at 460 nm, 0.8 μs after the 355 nm laser flash.

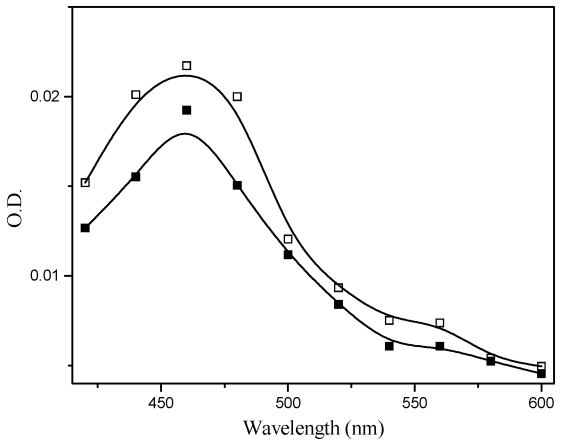

Figure 6. Transient absorption spectra of PZ (1×10^{-4} M)−DMDPM (2×10^{-2} M) at 0 T (■) and 0.1 T (□) in 0.2 M BHDC reverse micelle at $W_0 = 10$, 0.8 μs after the laser flash of 355 nm.

a large distance of separation (large W_0 values), spin correlation will be lost. So MFE requires an optimum separation between the participating RIPs that is attained at an intermediate W_0. However this optimum W_0 is not the same for all the acceptor−donor systems studied. This can again be explained by the preferential location of the amines in the reverse micelle as a result of which they are affected to different extents by the change in W_0. Although previously Uehata et al. have reported a decreasing field effect for the nonlinked zinc tetraphenylporphinate−viologen system, with increase in the water pool size[17] due to decrease in electron spin interaction in larger water pools, this is the first report of maximization of MFE at an intermediate W_0.

In BHDC, the MFE is prominent only for the PZ−DMDPM system. In this case as well MFE at $W_0 = 10$ (water pool size 20 Å) > MFE at $W_0 = 20$ (water pool size 40 Å). The MFE on the transient absorption of this system is shown in Figure 6. For the other acceptor−donor pairs, the field effect is not very apparent. This may be due to the electrostatic effect as explained above. Only DMDPM is suitably positioned to show MFE. The other RIPs are not efficiently separated.

In general the MFE in reverse micelles is much smaller compared to the MFE in micelles for all the systems studied. This may be due to the partitioning of the molecules between the organic and micellar phases. Only those molecules, which are trapped in the reverse micelle, are capable of responding to the magnetic field.

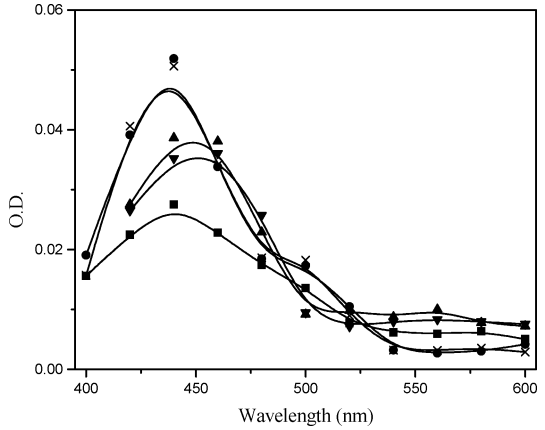

Figure 7. Transient absorption spectrum of PZ (1×10^{-4} M) (●), PZ (1×10^{-4} M)−DMA (8×10^{-3} M) (▲), PZ (1×10^{-4} M)−DEA (8×10^{-3} M) (▼), PZ (1×10^{-4} M)−DMDPM (7.2×10^{-4} M) (■), and PZ (1×10^{-4} M)−TEA (8×10^{-3} M) (×) in 0.01 M DMPC SUVs at 0.8 μs after the laser flash with excitation wavelength 355 nm.

MFE in SUVs. In SUVs, phospholipids form a bilayer in which the charged headgroups (zwitterionic in case of DMPC) are exposed to the internal entrapped water core and the outer water phase. SUVs thus have three well-defined zones: the entrapped water core, the bilayer, and the exterior bulk water.[8] So SUVs are frequently used as membrane mimetic systems. There have been some studies on PET in SUVs. Mataga and co-workers have employed the pyrene−DMA system in DMPC SUVs and suggested that the interior of the lipid bilayer is highly polar.[44] The fluorescence quenching of pyrene and 10-pyrenedecanoic acid by various anilines has also been investigated in dipalmitoylphosphatidylcholine SUVs.[45] MFE studies in SUVs are very few. Barra et al. have reported MFE on the photodecomposition of 1,1,3,3-tetraphenylacetone and 1,1-diphenylacetone in dioctadecyldimethylammoniumchloride vesicles.[20] Shafirovich et al. have used the MFE on the Zn porphyrin−viologen linked system to monitor molecular dynamics and probe phase transitions in SUVs.[19] To the best of our knowledge this is the first report of MFE on intermolecular PET reactions in SUVs.

Figure 7 shows the transient absorption spectra of all the systems in DMPC SUVs. The radical ion species are all distinctly observed. Figure 8 shows the MFE on the transient absorption for PZ−DMA, PZ−DEA, and PZ−DMDPM, respectively. No MFE is observed for PZ−TEA. PZ−DMA and PZ−DEA show a very small effect. The MFE is most prominent for the PZ−DMDPM system.

This can again be explained by the hydrophobicity and the preferential location of the amines. TEA, DMA, and DEA are less hydrophobic with the hydrophobicity increasing in that order and should be located in the hydrocarbon region near the headgroup of the lipid. It has been shown earlier that pyrene fluorescence is quenched by *p*-isopropyl-*N*,*N*-dimethylaniline to a greater extent than DMA in dipalmitoylphosphatidylcholine SUVs and this was attributed to the lower penetration of DMA inside the lipid bilayer.[45] Moreover, since EtOH solutions of these amines were added during preparation of these samples, there is a tendency for these molecules to remain in the aqueous phase. Only those molecules that are sequestered in the bilayer can be affected by a magnetic field, so a small MFE is observed. DMDPM cannot remain in the aqueous phase. We could not solubilize DMDPM beyond 7.2×10^{-4} M during SUV preparation, so whatever little DMDPM is present goes to the hydrophobic bilayer. Despite the lower concentration of DMDPM compared to the other amines, a pronounced MFE is

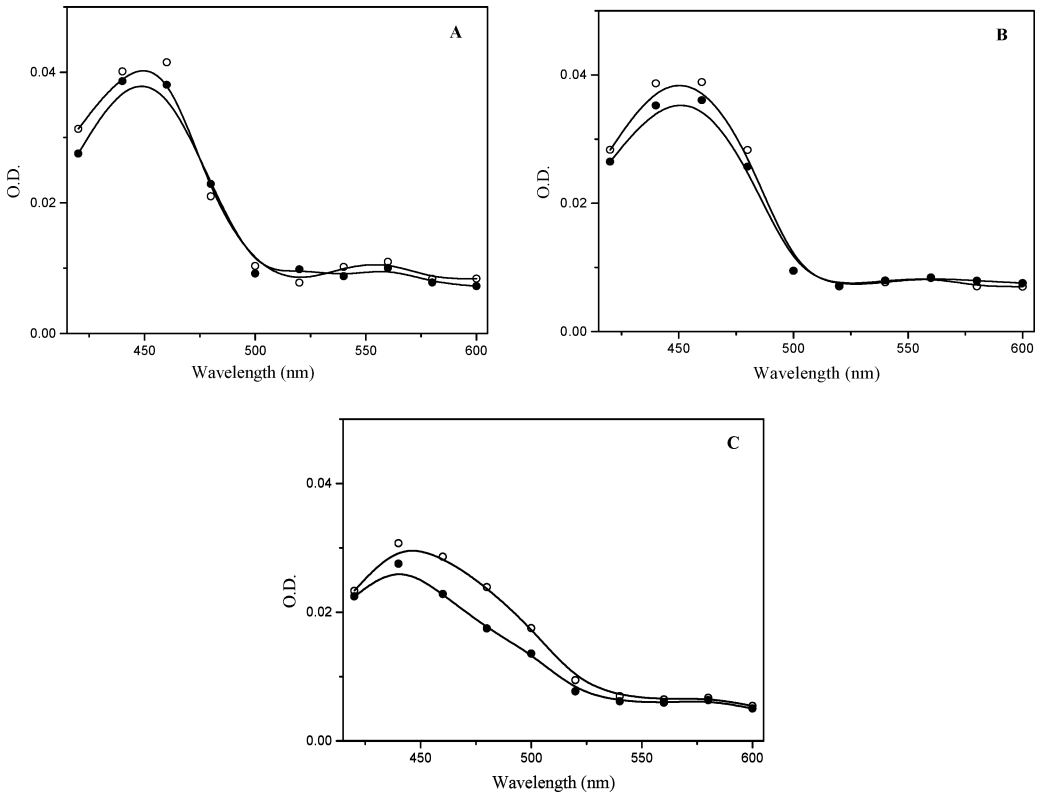

Figure 8. Transient absorption spectra of (A) PZ (1×10^{-4} M)−DMA (8×10^{-3} M), (B) PZ (1×10^{-4} M)−DEA (8×10^{-3} M), and (C) PZ (1×10^{-4} M)−DMDPM (7.2×10^{-4} M) in 0.01 M DMPC SUVs at 0 T (●) and 0.1 T (○) at 0.8 μs after the laser flash with excitation wavelength 355 nm.

observed. The lower concentration is also the reason for the low absorbance of $DMDPM^{\bullet+}$ (Figure 7).

MFE in Micelles, Reverse Micelles, and SUVs: A Comparison. The purpose of using organized assemblies in this work is twofold. Organized assemblies create a restricted environment for caging and thereby increase the lifetime of the transient species so that MFE is observable. This role is efficiently fulfilled by micelles, reverse micelles, and SUVs. However, these organized assemblies are structurally very different and have separate zones where the substrate molecules can be entrapped. So they help us to probe the effect of spatial partitioning on the magnetic field behavior. It is expected that there will be some differences in the behavior of the organized assemblies, and our studies have helped to elucidate these differences.

Figures 1, 4, and 7 show that the absorption by the radical ions and hence the yield of radical ions is more in SUVs and reverse micelles (anionic) compared to micelles. This indicates that the caging of the substrate inside the micelle is more efficient, whereas in reverse micelles and SUVs the mobility is higher and there is partitioning of the species within the organized assembly. This is also reflected in the magnetic field behavior. The MFE is much greater in micelles compared to reverse micelles and SUVs. The greater MFE in micelles allows us to perform studies with varying external magnetic fields, and these results also suggest that the donor and acceptor molecules are closely sequestered inside the micelle. Reverse micelles on the other hand provide a more open environment, and their size can be easily manipulated by varying W_0. This gives us the opportunity to explore the distance dependence of the MFE. Although the radical ion yield in SUVs is appreciable, the MFE is quite small. This again indicates that only a few molecules are trapped within the vesicle and capable of responding to the applied field.

CHART 1. Schematic Diagram Showing Partitioning of Species among Different Zones of the Organized Assemblies

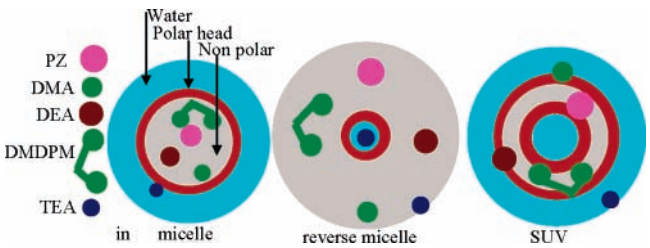

The partitioning of the species among the different zones of the organized assemblies in general depends on the bulk and hydrophobiciy of the individual species (Chart 1), and this in turn dictates their magnetic field behavior. TEA due to its small size and lower hydrophobicity shows very small or no MFE for all the systems studied. DMDPM, on the other hand, being bulky and hydrophobic is trapped and shows pronounced MFE in all the organized assemblies. DEA and DMA show intermediate behavior. Thus the MFE can be used to predict the nature of the participating molecules and their preferential location in an organized assembly.

Conclusion

This work illustrates the different magnetic field behavior of the various PZ−amine, acceptor−donor systems in micelles, reverse micelles, and SUVs. The amines are partitioned between the different phases of the organized assemblies depending on the bulk and hydrophobicity of the substituents. In general, the MFE is most prominent in micelles. The very high $B_{1/2}$ value indicates the role of hopping and lifetime broadening due to large effective concentration of the donors and the proximity

of the acceptor−donor pair. The RIP behavior in reverse micelles is guided by hydrophobic and electrostatic effects. MFE maximizes at an intermediate water pool size, W_0, which emphasizes the need for an optimum separation between the RIPs. In SUVs, the PZ−DMDPM system responds most strongly to the applied field because it is suitably positioned in the lipid bilayer. Thus our results show the importance of the structure of the organized assemblies on the dynamics of RIPs.

Acknowledgment. We are grateful to Prof. Nihar Ranjan Ray of Plasma Physics Division for kindly providing the Fluke combiscope and the Fluke View combiscope software. We thank Mrs. Chitra Raha for technical assistance. We also thank Mr. Hirak Chakraborty, Ms. Asima Chakraborty, and Miss Adity Chowdhury for their help.

References and Notes

(1) Steiner, U. E.; Ulrich, T. *Chem. Rev.* **1989**, *89*, 51 and references therein.
(2) Bhattacharya, K.; Chowdhury, M. *Chem. Rev.* **1993**, *93*, 507.
(3) *Dynamic spin chemistry magnetic controls and spin dynamics of chemical reactions*; Nagakura, S., Hayashi, H., Azumi, T., Eds.; Kodansha Ltd.: Tokyo, 1998.
(4) Gould, I. R.; Turro, N. J.; Zimmt, M. B. *Adv. Phys. Org. Chem.* **1984**, *20*, 1.
(5) Tanimoto, Y.; Fujiwara, Y. In *Handbook of photochemistry and photobiology Vol. 1: Inorganic Chemistry*; Nalwa, H. S., Ed.; American Scientific Publishers: Stevenson Ranch, CA, 2003.
(6) Staerk, H.; Weller, A.; Triechel, R.; Kuhnle, W. *Chem. Phys. Lett.* **1985**, *118*, 19.
(7) Weller, A.; Staerk, H.; Triechel, R. *Faraday Discuss. Chem. Soc.* **1984**, *78*, 271, 332.
(8) Fox, M. A. In *Topics in current chemistry*; Dewar, J. S., Dunitz, J. D., Hafner, K., Ito, S., Lehn, J. M., Neidenzu, K., Raymond, K. N., Rees, C. W., Vogtle, F., Eds.; Springer-Verlag: Heidelberg, Germany, 1991; Vol. 59.
(9) Dutta Choudhury, S.; Basu, S. *Chem. Phys. Lett.* **2003**, *373*, 67.
(10) Dutta Choudhury, S.; Basu, S. *Chem. Phys. Lett.* **2004**, *383*, 533.
(11) Turro, N. J.; Weed, G. C. *J. Am. Chem. Soc.* **1983**, *105*, 1861.
(12) Tanimoto, Y.; Shimizu, K.; Udagawa, H.; Itoh, M. *Chem. Lett.* **1983**, *13*, 353.
(13) Tanimoto, Y.; Takayama, M.; Itoh, M.; Nakagaki, R.; Nagakura, S. *Chem. Phys. Lett.* **1986**, *129*, 414.
(14) Schlenker, W.; Ulrich, T.; Steiner, U. E. *Chem. Phys. Lett.* **1983**, *103*, 118.
(15) Ulrich, T.; Steiner, U. E. *Chem. Phys. Lett.* **1984**, *112*, 365.
(16) Baumann, D.; Ulrich, T.; Steiner, U. E. *Chem. Phys. Lett.* **1987**, *137*, 113.
(17) Uehata, A.; Nakamura, H.; Usui, S.; Matsuo, T. *J. Phys. Chem.* **1989**, *93*, 8197.
(18) Parui, P. P.; Nath, D. N.; Chowdhury, M. *Chem. Phy. Lett.* **2004**, *396*, 329.
(19) Shafirovich, V. Y.; Batova, E. E.; Levin, P. P. *J. Am. Chem. Soc.* **1995**, *117*, 6093.
(20) Barra, M.; Bohne, C.; Zanocco, A.; Scaiano, J. C. *Langmuir* **1992**, *8*, 2390.
(21) *Reverse Micelles*; Luisi, P. L., Straub, B. E., Eds.; Plenum Press: New York, 1984.
(22) Luisi, P. L.; Giomini, M.; Pileni, M. P.; Robinson, B. H. *Biochim. Biophys. Acta* **1988**, *947*, 209.
(23) Silber, J. J.; Biasutti, A.; Abuin, E.; Lissi, E. *Adv. Colloid Interface Sci.* **1999**, *82*, 189.
(24) Huang, C. *Biochemistry* **1969**, *8*, 344.
(25) Ogata, T.; Yamamoto, Y.; Wada, Y.; Murakoshi, K.; Kusaba, M.; Nakashima, N.; Ishida, A.; Takamuku, S.; Yanagida, S. *J. Phys. Chem.* **1995**, *99*, 11916.
(26) Shida, T.; Hamill, W. H. *J. Chem. Phys.* **1966**, *44*, 2369.
(27) Ghosh, H. N.; Pal, H.; Sapre, A. V.; Mittal, J. P. *J. Am. Chem. Soc.* **1993**, *115*, 11722.
(28) Aich, S.; Basu, S. *J. Chem. Soc., Faraday Trans.* **1995**, *91*, 1593.
(29) Aich, S.; Basu, S. *J. Phys. Chem. A* **1998**, *102*, 722.
(30) Atik, S. S.; Thomas, J. K. *J. Am. Chem. Soc.* **1981**, *103*, 3550.
(31) Reiss-Husson, F.; Luzzati, V. *J. Phys. Chem.* **1964**, *68*, 3504.
(32) Wakasa, M.; Hayashi, H.; Mikami, Y.; Takeda, T. *J. Phys. Chem.* **1995**, *99*, 13181.
(33) Nolting, F.; Staerk, A.; Weller, A. *Chem. Phys. Lett.* **1982**, *88*, 523.
(34) *Landolt-Bornstein-Group II Molecules and Radicals*; Springer-Verlag: Heidelberg, Germany, 1992.
(35) Kruger, H. W.; Michel-Beyerle, M. E.; Knapp, E. W. *Chem. Phys.* **1983**, *74*, 205.
(36) Sakaguchi, Y.; Hayashi, H. *Chem. Phys. Lett.* **1982**, *87*, 539.
(37) Ulrich, T.; Steiner, U. E. *Chem. Phys. Lett.* **1984**, *112*, 365.
(38) Scaiano, J. C.; Joanovic, S. V.; Morris, D. G. *J. Photochem. Photobiol., A* **1998**, *113*, 197.
(39) Kikuchi, K.; Thomas, J. K. *Chem. Phys. Lett.* **1988**, *148*, 245.
(40) Geladé, E.; Boens, N.; De Schryver, F. C. *J. Am. Chem. Soc.* **1982**, *104*, 6288.
(41) Borsarelli, C. D.; Cosa, J. J.; Previtali, C. M. *Langmuir* **1992**, *8*, 1070.
(42) Borsarelli, C. D.; Cosa, J. J.; Previtali, C. M. *Photochem. Photobiol.* **1998**, *68*, 438.
(43) Borsarelli, C. D.; Cosa, J. J.; Previtali, C. M. *Photochem. Photobiol.* **2001**, *73*, 97.
(44) Waka, Y.; Mataga, N.; Tanaka, F. *Photochem. Photobiol.* **1980**, *32*, 335.
(45) Kano, K.; Kawazumi, H.; Ogawa, T.; Sunamoto, J. *Chem. Phys. Lett.* **1980**, *74*, 511.